Inverse Problems in Science and Engineering
Vol. 17, No. 2, March 2009, 175–186

Taylor & Francis
Taylor & Francis Group

Projected gradient methods for synchrotron radiation spectra distribution function reconstruction

Yanfei Wang[a]*, Yonghua Du[bc] and Tiandou Hu[b]

[a]*Institute of Geology and Geophysics, Chinese Academy of Sciences, Beijing, P.R. China;*
[b]*Institute of High Energy Physics, Chinese Academy of Sciences, Beijing, P.R. China;*
[c]*Graduate University of Chinese Academy of Sciences, Beijing, P.R. China*

(*Received 16 April 2007; final version received 30 November 2007*)

The theory of synchrotron radiation (SR) has been well understood and published. We study the numerical methods for the reconstruction of the spectral distribution function of SR by measurement of the attenuation of the SR energy spectrum. The reconstruction of the spectral distribution function of SR is an ill-posed integral operator equation of the first kind. Therefore, how to overcome the ill-posedness is a major task in numerical computation. We study the projected gradient methods and propose a non-monotone decreasing algorithm, which is called the projected Barzilai-Borwein (PBB) method. The feasibility of the method is studied in detail by using a hypothetical SR spectrum. The applied results of the spectrum of 4W1B beamline (an unfocused X-ray monochromator beamline with 4 mrad (milliradian) of horizontal acceptance which is extracted from the wavelength shifter 4W1) in BSRF (Beijing Synchrotron Radiation Facility) are shown.

Keywords: synchrotron radiation (SR); projected gradient methods; numerical inversion; X-ray attenuation

Downloaded By: [Wang, Yanfei] At: 02:34 11 February 2009

1. Introduction

The synchrotron radiation (SR) is emitted by electrons orbiting in a storage ring. It provides X-rays which are used for a wide range of analytical techniques. Since SR was first observed in 1947, it has been applied to many fields due to its good characteristics, and the theory of SR has been well understood and published [1–3]. One of the important characteristics is that the spectrum of SR source can be accurately calculated. So we often get the SR spectrum by theoretical calculation instead of experimental measurement. But, in reality, the feasibility of calculation is affected by many factors, for example, fluctuations of the parameter of insertion devices and the electron orbit, the change of acceptance angle. On the other hand, usually we are interested in the spectral distribution at the samples. The spectrum will be changed when the light transmits some optical elements in the beamline. Due to the above reasons, the experimental measurement of spectrum of SR is important in practice.

*Corresponding author. Email: yfwang_ucf@yahoo.com

ISSN 1741–5977 print/ISSN 1741–5985 online
© 2009 Taylor & Francis
DOI: 10.1080/17415970802082781
http://www.informaworld.com

Some methods, such as monochromatization, detectors with energy resolution and attenuation filters, have been developed to measure the X-ray spectrum. But each of these methods has its own shortcomings. For the monochromatization method, the energy range of the monochromator is limited and the real diffraction efficiency of the crystal is hard to confirm, which makes an exact calculation unfeasible. Another common method is to measure directly by solid detector with energy resolution. In order to avoid the detector becoming saturated, some kind of scatterer is always needed. This method overcomes the problem of energy limitation, but the complex scattering problem and the detector response have to be taken into account.

The conventional X-ray attenuation experiments were done by adding separated filtrations with different thickness in the light path. It is hard to reconstruct the spectral distribution accurately because only a few discrete data can be collected by this method. In order to obtain enough data easily, we adopt a wedged filtration. The filtration was driven by a step motor and at the same time its thickness was changed. Experiments were done at 4W1B beamline in the Beijing Synchrotron Radiation Facility (BSRF). SR was extracted at the straight section of 4W1 of the BSRF with an electromagnetic wiggler. Details of our experimental setup, and experimental geometry and components have already been given in [4]. The principle of our experiment is the detection of the attenuation of SR light and solving an inverse problem.

Downloaded By: [Wang, Yanfei] At: 02:34 11 February 2009

Attenuation filter is a simple method in experiment. But reconstructing the real spectrum is a difficult task because it requires an ill-posed inverse problem to be solved. The earliest method was an analytical approach using a Laplace transform for representing the X-ray spectral distributions in a function form [5]. Later, various techniques for both direct computation and iterative computation were developed [6–12], however the computational results of those methods are not satisfactory. In inversion theory, regularization methods play an important role in stably recovering the unknowns given that the observations are known, which has been applied successfully in a lot of fields such as geophysics, computerized tomography, signal and image processing [13] and Laplace transform [14,15]. It is a powerful tool for solving operator equations of the first kind. Recently, we have applied the Tikhonov regularization method under some conditions to reconstruct the SR spectra radiation function and obtain satisfactory results. However, this method still relies heavily on the proper choice of the regularization parameter and the stabilizer [4]. It is not convenient sometimes, for example, if *a priori* information about the noise level is unavailable. Therefore, more robust algorithms deserve to be studied. We study gradient methods in this article, which correspond to some kind of regularization if proper controlling of the iterations is done. Particularly, we study the projected Barzilai-Borwein (PBB) method in a convex and closed feasible set and apply it to rebuild the spectrum of SR. The method originates from solving a well-posed non-linear programming problem [16], but it is the first time it has been used for solving an ill-posed SR spectra distribution function reconstruction problem. In addition, a projection technique for box-constrained optimization of this problem is presented. These results, which in essence are the main contributions of the article, are the pivotal points for the effectiveness of the numerical procedure based on the projected gradient method in BB type analysed in this article. Numerical experiments on both theoretical and practical simulations are performed.

The structure of the article is as follows: in Section 2, we outline the model as an integral operator equation of the first kind; in Section 3, we first briefly introduce the regularization method, then describe the projected gradient methods and propose a PBB

method in detail; in Section 4, numerical experiments are given for both theoretical and practical simulations. Finally in Section 5, some concluding remarks are given.

2. Mathematical model: ill-posed integral equations of the first kind

When SR with spectrum distribution $f(E)$ traverse the filtration, the intensity is attenuated. The signal obtained by the second ion chamber is

$$I(d) = a\int_{E_0}^{E_1} f(E)e^{-\mu(E)d}E[1 - e^{-\mu_g(E)D}]\mathrm{d}E, \tag{2.1}$$

where E is the energy of the light, $\mu(E)$ is the absorption coefficient of the filtration, $\mu_g(E)$ is the absorption coefficient of the gas filled in the chamber, d is the thickness of the filtration, D is the length of the ion chamber, E_0 and E_1 are, respectively, the minimum and maximum photon energy of the incident light. Here, $a = Gq/\varepsilon_{\mathrm{ion}}$. G is the gain of the amplifier, q is the electron charge, $\varepsilon_{\mathrm{ion}}$ is the ionization energy of the gas filled in the chamber.

Considering the wedged filtration and the width of the beam, Equation (2.1) has to be corrected, i.e.

$$I(d) = a\int_{E_0}^{E_1} \frac{f(E)[1 - e^{-\mu(E)w\tan(\theta)}]}{\mu(E)w\tan(\theta)}E[1 - e^{-\mu_g(E)D}]e^{-\mu(E)d}\,\mathrm{d}E, \tag{2.2}$$

where w is the width of the light, θ is the apex angle of the filtration.

By variable replacement, Equation (2.2) can be rewritten as

$$I(d) = a\int_{\mu_0}^{\mu_1} g(\mu)e^{-\mu d}\,\mathrm{d}\mu, \tag{2.3}$$

where

$$g(\mu) = \frac{f[E(\mu)]E(\mu)e^{-\mu_g E(\mu)D}[1 - e^{-\mu w\tan(\theta)}]}{\mu w\tan(\theta)}\frac{\mathrm{d}E}{\mathrm{d}\mu}.$$

It is clear that (2.3) is a Laplace integral equation, which is a special operator equation of the first kind, hence the ill-posed nature it inherits. This means that even if a least squares solution with minimal norm in L_2 space exists, it may oscillate severely with the perturbation of the observation. So, direct solution of (2.3) or finding its least square errors (LSE) solution should be avoided. To see this, first we formulate the problem in the Hilbert space:

$$L : \mathcal{F} \to \mathcal{R}$$
$$(Lg)(\mu) = I(d),$$

where $\mathcal{F}$ and $\mathcal{R}$ are two Hilbert spaces, whose norm is induced by inner product and $g \in \mathcal{F}$, $I \in \mathcal{R}$.

If we denote the singular system of L by $\{\sigma_k; u_k, v_k\}$, then the singular value expansion of L can be expressed as

$$Lu_k = \sigma_k v_k, \quad L^* v_k = \sigma_k u_k$$

Downloaded By: [Wang, Yanfei] At: 02:34 11 February 2009

and

$$Lg = \sum_{k=1}^{\infty} \sigma_k(g, u_k)v_k, \quad g \in \mathcal{F},$$

$$L^*I = \sum_{k=1}^{\infty} \sigma_k(I, v_k)u_k, \quad I \in \mathcal{R}.$$

where L^* is the adjoint of L. With the singular value expansion of the operator L, the solution of the LSE problem can be approximated by

$$g^{lse} = L^{\dagger}I = (L^*L)^{\dagger}L^*I = \sum_{k=1}^{\infty} \frac{(I, v_k)}{\sigma_k} u_k,$$

where $L^{\dagger}$ is the Moore–Penrose generalized inverse.

Note that L is an ill-posed operator, hence $L^{\dagger}$ is unbounded if the dimension of the range of the observation space is infinity. This indicates that g^{lse} is very sensitive to the observations in $\mathcal{R}$ and the instability occurs.

Downloaded By: [Wang, Yanfei] At: 02:34 11 February 2009

3. Numerical methodology

3.1. *Regularization methods*

Due to the ill-posedness of (2.3), some kind of regularization technique must be involved to suppress the ill-posed characteristic [14,15,17,18]. One may readily see that a proper filter function to suppress the instability induced by the small singular values and noise data should be considered. If we choose the filter function to have the terms containing small singular values truncated, then we obtain the truncated singular value decomposition [18]. The Tikhonov regularization technique is another choice of filter function. The standard Tikhonov regularization refers to solving an unconstrained minimization problem [15,19,20]

$$\|Lg - I\|_{L_2}^2 + \alpha\Omega(g) \rightarrow \text{minimization}, \tag{3.1}$$

where $\Omega(g)$ is called the stabilizer, and the functional $\Omega(\cdot)$ can be defined by users. For example, $\Omega(\cdot)$ can be chosen as $\|\cdot\|_{W_2^1}$, a normed space in the Sobolev space, which means the function g is continuous and differentiable with the bounded norms of itself and its generalized derivatives in L_2. If we choose $\Omega(\cdot)$ as $\|\cdot\|_{L_2}$, then we obtain the regularized solution as

$$g^{\alpha} = (L^*L + \alpha E)^{-1}L^*g,$$

where E is the identity operator. This is equivalent to choosing the filter function as $(\sigma^2/\alpha + \sigma^2)$. α is the so-called regularization parameter which is greater than 0. The choice of α is a delicate thing, which plays a vital role in the regularization process. Therefore, for regularization methods, one needs to impose a regularized term with a proper choice of regularization parameter α. However, it is hard to make the best choice in practice if *a priori* information about the noise level is unavailable. To avoid difficulties, we consider projected gradient methods in this article.

3.2. *Projected gradient methods*

Equation (2.3) is a bounded Laplace transform for our detection system. Numerically, rewriting Equation (2.3) in discrete form yields $y = Kx$. In which, y and x are column vectors with the dimensions of m and n, respectively, and K is an $m \times n$ matrix. They are defined as follows:

$$y = \begin{bmatrix} I(d_1) \\ \vdots \\ I(d_m) \end{bmatrix}, \quad x = \begin{bmatrix} g(\mu_1) \\ \vdots \\ g(\mu_n) \end{bmatrix}, \quad K = a\Delta\mu \begin{bmatrix} e^{-\mu_1 d_1} & \dots & e^{-\mu_n d_1} \\ \vdots & \vdots & \vdots \\ e^{-\mu_1 d_m} & \dots & e^{-\mu_n d_m} \end{bmatrix}. \tag{3.2}$$

Gradient methods are used for functional minimization. Every one of them uses an iterative formula that contains the gradient of the functional to find the minimum, hence the name 'gradient methods'. The problem is defined by the functional to be minimized and the initial approximation, the starting point for the iteration. The method stops when the maximum number of iterations is exceeded or the requested accuracy is obtained for the solution. More than one method can be used for the same problem. Now we turn to the minimization of a function of n variables:

$$J[x] := \frac{1}{2} x^T A x - b^T x, \tag{3.3}$$

where $A = K^T K$, $b = K^T y$. Let x_k be the k-th iterate and $\text{grad}_k[J]$ the gradient of J at x_k, given by

$$\text{grad}_k[J] = Ax_k - b.$$

A gradient method for solving (3.3) calculates the next point from

$$x_{k+1} = x_k + \alpha_k d_k,$$

where $d_k = -\text{grad}_k[J]$ is the negative gradient direction, α_k is the stepsize that depends on the method used. For example, for the classical steepest descent (SD) method [21], the stepsize α_k is chosen such that $J[x]$ is minimized along the line $x_k - \alpha_k \text{grad}_k[J]$, that is,

$$\alpha_k^{SD} = \text{argmin}_{\alpha > 0} J[x_k - \alpha \, \text{grad}_k[J]],$$

which leads to the solution

$$\alpha_k^{SD} = \frac{\text{grad}_k[J]^T \text{grad}_k[J]}{\text{grad}_k[J]^T A \, \text{grad}_k[J]}.$$

Theoretically, the solution of problem (2.3) is bounded and positive, so is problem (3.2). That is to say, the solution x belongs to a convex and closed set $\Omega = \{x \in \mathbb{R}^n : l \le x \le u, \ l \ge 0, \ u < \infty\}$, and l, u are all vectors in $\mathbb{R}^n$. Therefore, we actually solve a constrained optimization problem:

$$\begin{aligned} &\min J[x] := \frac{1}{2} x^T A x - b^T x, \\ &\text{subject to } x \in \Omega. \end{aligned} \tag{3.4}$$

Convexity of Ω makes it possible to use the orthogonal projection onto Ω, $P_\Omega : \mathbb{R}^n \to \Omega$, for obtaining feasible directions which are also descent ones; namely a step is taken from

Downloaded By: [Wang, Yanfei] At: 02:34 11 February 2009

x_k in the direction of $-\text{grad}_k[J]$, the resulting vector is projected onto Ω, and the direction from x_k to this projection has the above mentioned properties. Ideally, the projection P_Ω should be chosen such that

$$P_\Omega(x) = \text{argmin}_z \|x - z\|.$$

For our problems with $l \geq 0$ and $u < \infty$, we choose the projection operator on Ω as

$$P_\Omega(x) = \max(x, 0)$$

and the i-th component of P_Ω can be expressed simply as

$$P^i_\Omega(x) = \begin{cases} x_i & \text{if } x_i \geq 0, \\ 0 & \text{otherwise.} \end{cases}$$

Assume that the current iterate x_k is feasible, then the next iteration point can be obtained by

$$x_{k+1} = P_\Omega(x_k - \alpha_k \text{grad}_k[J]). \tag{3.5}$$

We outline the projected gradient algorithm as follows:

Algorithm 1 (Projected gradient algorithm)

- Initialization: Give $x_0 \in \Omega$ and the stopping tolerance ϵ;
- Iteration: If $\|\text{grad}_k[J]\| \leq \epsilon$, then stop. Otherwise, solve Equation (3.5) to obtain the next iterate x_{k+1}.

Shortcomings of this method are that it becomes slow as the iterations proceed, and zigzagging phenomenon occurs [21]. So, it is not applicable in practical applications.

Another iterative projected gradient method is the projected Landweber method, which is proposed by Eicke [22], for solving convexly constrained ill-posed problems in the Hilbert space. This method is also addressed in [23]. The iteration formula reads as follows:

$$\begin{aligned} x_{k+1} &= P_\Omega\big(x_k + \omega\big(K^T y - K^T K x\big)\big) \\ &= P_\Omega(x_k + \omega(b - A x_k)) \\ &= P_\Omega(x_k - \omega \,\text{grad}_k[J]) \end{aligned} \tag{3.6}$$

where $\omega \in (0,\ \|A\|^{-2})$, $P_\Omega(\cdot)$ is the projection operator defined as above. The projected Landweber method is an iterative method which can be used for approximating the solutions of the image restoration problems. Its convergence and regularization properties have been investigated in [22]. However, a well-known fact is the practical difficulty of the method, i.e. the convergence is too slow. Too many iterations are required to obtain the best approximation. Therefore, if one wants to use the method, the acceleration technique must be considered. But how to accelerate remains an important issue.

Recently, a new method for the choice of stepsize α_k, called the BB method was proposed by Barzilai and Borwein [16] for solving unconstrained quadratic programming problems. Applications of the method to a digital image restoration problem are reported in [24]. This method is based on the investigation of the quasi-Newton equation of Equation (3.3)

$$A\Delta x_{k-1} = \Delta \text{grad}_{k-1}[J],$$

Downloaded By: [Wang, Yanfei] At: 02:34 11 February 2009

where $\Delta x_{k-1} = x_k - x_{k-1}$, $\Delta \text{grad}_{k-1}[J] = \text{grad}_k[J] - \text{grad}_{k-1}[J]$ and minimizing the norm of the residual $\Delta \text{grad}_{k-1}[J] - A\Delta x_{k-1}$ for A approximated by $\alpha^{-1}I$ ($\alpha > 0$, I is the identity matrix). This yields two choices of the stepsize α_k:

$$\alpha_k^{BB1} = \frac{\text{grad}_{k-1}[J]^T \text{grad}_{k-1}[J]}{\text{grad}_{k-1}[J]^T A\, \text{grad}_{k-1}[J]}, \tag{3.7}$$

$$\alpha_k^{BB2} = \frac{\text{grad}_{k-1}[J]^T \text{grad}_{k-1}[J]}{\text{grad}_{k-1}[J]^T A^2\, \text{grad}_{k-1}[J]}. \tag{3.8}$$

The PBB method refers to choosing α_k in Equation (3.5) as α_k^{BB1} in (3.7) or α_k^{BB2} in (3.8) or a combination of both, then implementing Algorithm 1 until finding a satisfactory solution. This method which has been seen to perform well for the quadratic model in numerical optimization [25,26] and for ill-posed digital image restoration problems [24]. A remarkable feature of the PBB method is its non-monotonicity in iterations. In addition, this method can avoid negative values in the iterations. We will use this method for recovering SR spectra distribution function. For stopping criterion, we adopt the stopping condition (suggested in [24] for ill-posed problems) in our numerical tests:

$$\|\widetilde{\text{grad}}_k[J]\| \le \varepsilon \|\text{grad}_1[J]\|, \tag{3.9}$$

where ε is a preassigned tolerance and $\widetilde{\text{grad}}_k[J]$ is defined as

$$(\widetilde{\text{grad}}_k[J])_i = \begin{cases} (\text{grad}_k[J])_i & \text{if } (x_k)_i > 0, \\ \min\{(\text{grad}_k[J])_i, 0\} & \text{if } (x_k)_i = 0. \end{cases}$$

Its numerical performances are illustrated in next section.

4. Numerical experiments

4.1. *Theoretical simulation*

In order to test the stability and reliability of the algorithm, we first generate a theoretical spectral distribution according to the parameters of 4W1B beamline in BSRF, which is illustrated in Figure 1(b) (solid line). The energy range of the object distribution is from 4 KeV to 30 KeV. The material for attenuation is Al whose thickness was chosen from 0 to 10 mm and the absorption coefficients were quoted from [27]. Figure 1(a) shows the attenuation curve without noise.

Applying our algorithm to the attenuation curve without noise, we get the numerical inversion results. Recalling the stopping rule in Algorithm 1 is based on the norm of the gradient, i.e. the iterations should be stopped once $\|\widetilde{\text{grad}}_k[J]\| \le \varepsilon \|\text{grad}_1[J]\|$ is satisfied. In this noise-free simulation, the tolerance ε is chosen as 1.0×10^{-7}. In Figure 1(b), the solid line is the object spectrum and the circles are the numerical inversion results. The errors between the object and the results are shown in Figure 1(c). The error limit is $< 1.40 \times 10^{-6}$. The behaviour of the relative error of the PBB method in each iteration is shown in Figure 1(d). It can be clearly seen from Figure 1(d) that the relative error does

Downloaded By: [Wang, Yanfei] At: 02:34 11 February 2009

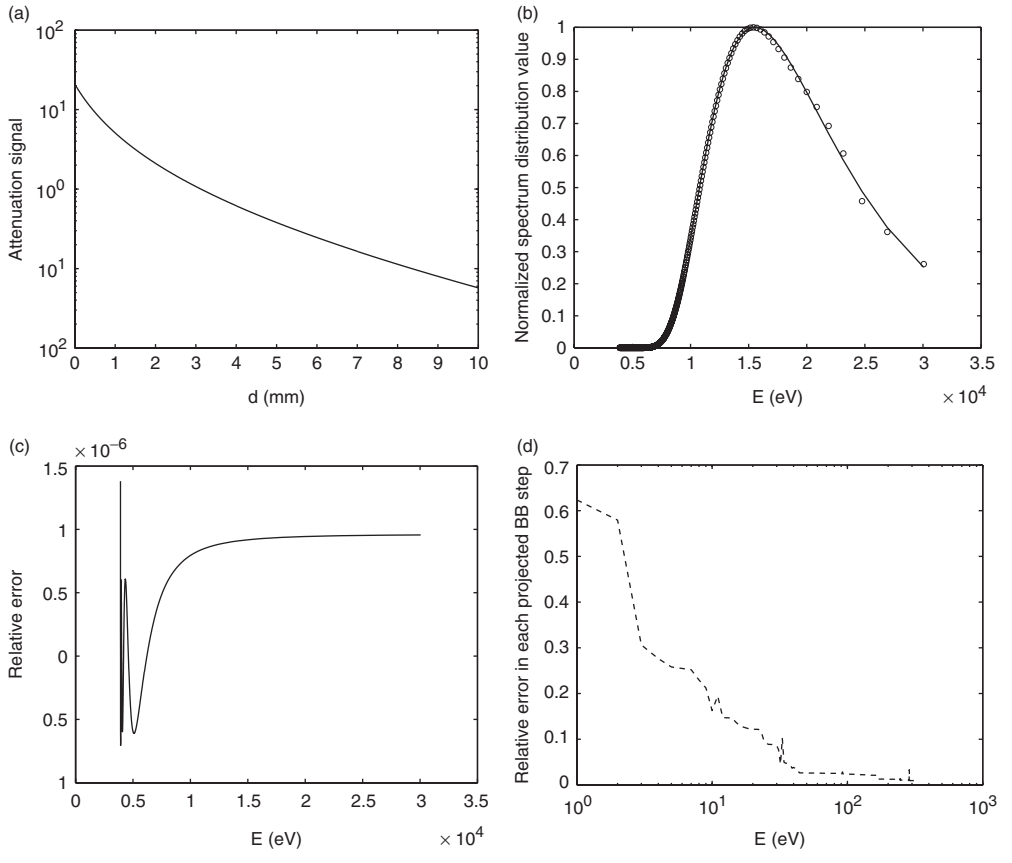

Figure 1. (a) The simulated attenuation curve without noise. (b) The solid line is the object distribution, the circles are the numerical inversion results from the unperturbed simulated attenuation data. (c) The relative error between the object spectrum and the numerical inversion results from the simulated attenuation data without noise. (d) The behaviour of the relative error for the PBB method.

Downloaded By: [Wang, Yanfei] At: 02:34 11 February 2009

not decrease monotonically due to the non-monotonicity of the PBB method. The numerical results show that the algorithm is successful when the data have no noise.

In order to test the anti-noise capability of the algorithm, a Gaussian random white noise in $[-1, 1]$ with a high level 0.05 (i.e. 0.05 times the Gaussian random white noise) was added to the simulated attenuation curve. The tolerance $\varepsilon = 1.0 \times 10^{-6}$ is used in this case. In our simulation process, the effects of the noise to the simulated attenuation curve can be seen clearly in the partial enlarged detail. Figure 2(b) (solid line) shows the object spectrum.

The numerical inversion results from the noisy attenuation curve are shown in Figure 2(b) (circles). The errors between the true and the computational results are shown in Figure 2(c). The error limit is $<0.032\%$. It indicates that the numerical inversion results and the object distribution are very similar even for high noise levels. This shows that our algorithm is stable and reliable. The behaviour of the relative error of the PBB method in each iteration is shown in Figure 2(d). Again, it can be seen from Figure 2(d) that the relative error does not decrease monotonically due to the non-monotonicity of the PBB method.

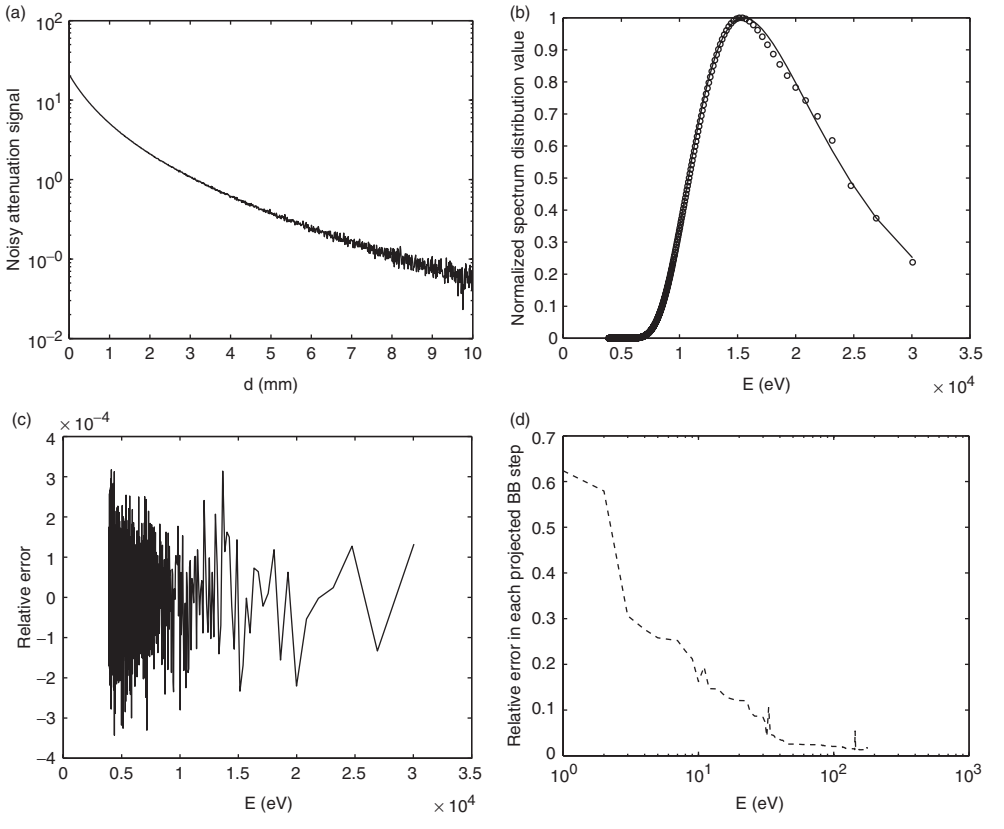

Figure 2. (a) The simulated attenuation curve is perturbed with Gaussian random white noise in [−1,1], the noise level 0.05. (b) The solid line is the object distribution. The circles are the numerical inversion results from the perturbed attenuation curve. (c) The relative error between the object spectrum and the numerical inversion results from the perturbed simulated attenuation data. (d) The behaviour of the relative error for the PBB method.

Downloaded By: [Wang, Yanfei] At: 02:34 11 February 2009

4.2. *Practical SR spectral distribution function recovery*

Next, we examine our algorithm for practical observation data. All experiments were done at 4W1B beamline in BSRF (see [4] for details). In our experiments, the thickness of the tip of the filtration is about 0.25 mm. It means that SR will be absorbed by an Al foil of 0.25 mm before we measure it. Therefore, in numerical comparison with the theoretical values, an 0.25 mm-thick Al is added. In our numerical tests, all curves are normalized by the maximum.

In our calculation, 1000 points were chosen from the measurements. To ensure convergence and sufficient iterations, the tolerance $\varepsilon = 2.5 \times 10^{-4}$ is used in this case. The inversion results are shown in Figure 3(a). The dotted line represents the numerical inversion results by using experiment data. The solid line denotes the theoretical distribution of the light in the centre of the cross section. Comparing with theoretical results and the calculation results, we find that our algorithm is believable for measured data.

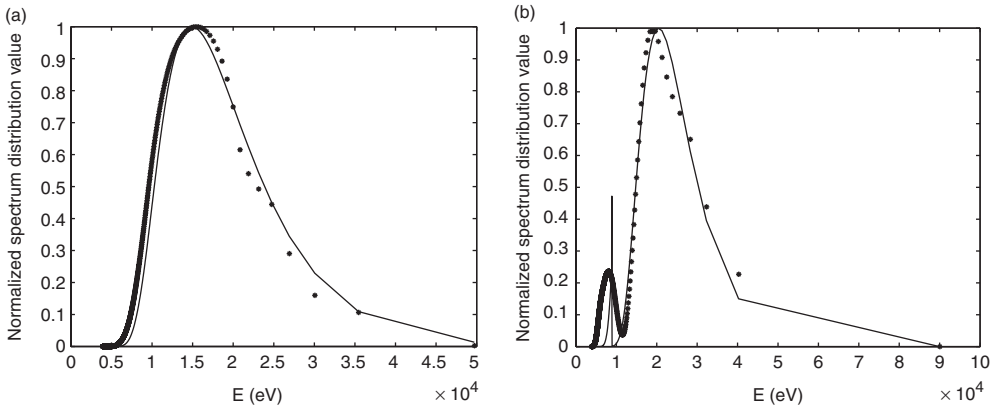

Figure 3. (a) The solid line is the theoretical distribution of the centre of the light. The * line represents the numerical inversion results from experimental data. (b) The solid line is the theoretical result of the white light absorbed by Cu. The * line denotes the numerical inversion results.

Downloaded By: [Wang, Yanfei] At: 02:34 11 February 2009

In order to check the reliability of the inversion algorithm, we have collected the data with 35 μm Cu in the light path. In this case, the tolerance is chosen as $\varepsilon = 1.0 \times 10^{-4}$. The spectrum with Cu absorption was reconstructed by the same algorithm. The result is shown in Figure 3(b). The solid line is the theoretical result of the white light absorbed by Cu and the dotted line is the numerical inversion results. We can clearly see the position of the absorption edge of Cu can be reconstructed. This indicates that the numerical results of the spectrum absorbed by Cu are reliable. Furthermore, it illustrates that the numerical results of white light are reliable.

Both the theoretical simulation and the inversion by measurement data reveal the fact that our method can stably and efficiently recover the SR spectra distribution function. Therefore, we conclude that our method is applicable for the inversion in the recovery of the SR spectra distribution function.

5. Concluding remarks

This article introduces a simple experimental method and a reliable projected gradient method to measure and reconstruct the spectrum of SR. The inversion algorithm was tested by theoretical spectral distribution. Several practical measurements were carried out at 4W1B beamline in BSRF, and the numerical results are illustrated to be reliable. To deal with the ill-posed problem described in this article, we propose projected gradient methods, particularly a PBB method for computing the non-monotone step in each iteration. Numerical performance reveals its good stability. Therefore, PBB method for ill-posed SR spectrum reconstruction problem with non-negative constraints corresponds to a kind of regularization. This regularization is ensured by the proper choice of the stopping rule and the stopping rule does not depend on the noise level. As is seen, the termination of the iteration process is controlled by the tolerance ε in the stopping condition (3.9). One may ask how to choose the tolerance ε? Empirically, we recommend ε to be chosen as in the order of $O(10^{-6})$ for synthetic data in theoretical simulations, and $O(10^{-4})$ for practical data. The stable algorithm and plenty of experimental data ensure

the reliability of reconstructed spectrum. This method can be used to measure the spectrum of X-ray.

Acknowledgements

We would like to express our sincere thanks to the anonymous referees' valuable suggestions which greatly help us improve the quality of the article. The research is sponsored by China National Natural Science Foundation 10501051 and partially supported by NSFC-RFBR project 10811120017.

References

[1] F.J. Himpsel and I. Lindau, *Photoemission and photoelectron spectra*, in *The Optics Encyclopedia*, Vol. 4, Th. G. Brown, K. Creath, H. Kogelnik, M.A. Kriss, J. Schmit, and M.J. Weber, eds., Wiley-VCH, Weinheim, 2004, pp. 2343–2370.

[2] M. Procop and F. Scholze, *Synchrotron radiation for the characterization of energy dispersive X-ray spectrometers*, Microsc. Microanal. 10(Suppl. S02) (2004), pp. 98–99.

[3] M. Servidori, *Determination by high-resolution X-ray diffraction of shape, size and lateral separation of buried empty channels in silicon-on-nothing architectures*, J. Appl. Cryst. 40 (2007), pp. 338–343.

[4] Y.H. Du, Y.F. Wang, W. Hua, Y.Y. Huang, and T.D. Hu, *Measurement of synchrotron radiation spectra using combined attenuation method and regularized inversion*, Nucl. Instrum. Meth. Phys. Res. A 565 (2006), pp. 855–860.

[5] L. Silverstein, *Determination of the spectral composition of X-ray radiation from filtration data*, J. Opt. Soc. Amer. 22 (1932), pp. 265–280.

[6] G.E. Bell, *Spectral distribution in the continuous X-ray spectrum and the specification of X-ray quality*, Brit. J. Radiol. 9 (1936), pp. 680–688.

[7] J.R. Greening, *The derivation of approximate X-ray spectral distributions and an analysis of X-ray 'quality' specifications*, Brit. J. Radiol. 36 (1963), pp. 363–371.

[8] H.M. Kramer and H. Von Seggern, *The determination of X-ray spectra from attenuation data*, Nucl. Instr. and Meth. 213 (1983), p. 373.

[9] B.W. Soole, *A method of X-ray attenuation analysis for approximating the intensity distribution at its point of origin of bremsstrahlung excited in a thick target by incident electrons of constant medium energy*, Phys. Med. Biol. 21 (1976), pp. 369–389.

[10] S. Tominaga, *The estimation of x-ray spectral distribution from attenuation data by means of iterative computation*, Nucl. Instr. Meth. 192 (1982), pp. 415–421.

[11] ——, *A singular-value decomposition approach to X-ray spectral estimation from attenuation data*, Nucl. Instr. Meth. A 243 (1986), pp. 530–538.

[12] J.W. Twidell, *The determination of X-ray spectra using attenuation measurements and a computer program*, Phys. Med. Biol. 15 (1970), pp. 529–539.

[13] Y.F. Wang, *Computational Methods for Inverse Problems and Their Applications*, Higher Education Press, Beijing, 2007.

[14] Y.F. Wang and T.Y. Xiao, *Fast realization algorithms for determinig regularization parameters in linear inverse problems*, Inverse Probl. 17 (2001), pp. 281–291.

[15] T.Y. Xiao, S.G. Yu, and Y.F. Wang, *Numerical Methods for Inverse Problems*, Science Press, Beijing, 2003.

[16] J. Barzilai and J. Borwein, *Two-point step size gradient methods*, IMA J. Numer. Anal. 8 (1988), pp. 141–148.

[17] H.W. Engl, M. Hanke, and A. Neubauer, *Regularization of Inverse Problems*, Kluwer, Dordrecht, 1996.

Downloaded By: [Wang, Yanfei] At: 02:34 11 February 2009

[18] C.R. Vogel, *Computational Methods for Inverse Problems*, SIAM, Philadelphia, 2002.
[19] A.N. Tikhonov and V.Y. Arsenin, *Solutions of Ill-posed Problems*, John Wiley and Sons, New York, 1977.
[20] A.N. Tikhonov et al., *Numerical Methods for the Solution of Ill-posed Problems*, Kluwer Academic Publishers, Dordrecht, 1995.
[21] Y.X. Yuan, *Numerical Methods for Nonliear Programming*, Shanghai Science and Technology Publication, Shanghai, 1993.
[22] B. Eicke, *Iteration methods for convexly constrained ill-posed problems in Hilbert space*, Num. Funct. Anal. Opt. 13 (1992), pp. 413–429.
[23] M. Bertero and P. Boccacci, *Introduction to Inverse Problems in Imaging*, Institute of Physics Publishing, Philadelphia, 1998.
[24] Y.F. Wang and S.Q. Ma, *Projected barzilai-borwein methods for large scale nonnegative image restorations*, Inverse Probl. Sci. Eng. 15 (2007), pp. 559–583.
[25] Y.H. Dai and R. Fletcher, *Projected Barzilai-Borwein methods for large-scale box-constrained quadratic programming*, University of Dundee Report NA/215, 2003.
[26] M. Raydan, *On the Barzilai and Borwein choice of steplength for the gradient method*, IMA J. Numer. Anal. 13 (1993), pp. 321–326.
[27] C.T. Chantler, *Theoretical form factor, attenuation and scattering tabulation for* $z = 1 - 92$ *from* $e = 1 - 10\,ev$ *to* $e = 0.4 - 1.0\,mev$, J. Phys. Chem. Ref. Data 24 (1995), pp. 71–643.

Downloaded By: [Wang, Yanfei] At: 02:34 11 February 2009